

NEW OPTIMIZATION FOR THE LCLS PHOTO-INJECTOR

C.Limborg*, J.Clendenin, D.Dowell, S.Gierman, J.Schmerge
Stanford Linear Accelerator Center, Stanford University, Stanford, CA 94309, USA

Abstract

A new parameter optimization of the LCLS photo-injector beamline minimizing the transverse emittance has been established for operating the gun at 120MV/m. The design goals of the LCLS photo-injector beamline are to provide a 150 MeV, 10ps FWHM, 1nC bunch at 120Hz with less than 1.2 mm.mrad for the projected emittance and less than 1 mm.mrad for the slice emittance for 80 slices out of 100. The new optimization gives 0.92 mm.mrad for the normalized projected emittance (ϵ_p) and less than 0.8 mm.mrad normalized slice emittances for 80 slices out of 100, for perfect beam conditions and with 0.7 ps rise time on the laser pulse and a 0.3mm.mrad thermal emittance (ϵ_{th}). Combining multiple errors on tuning parameters and emission pulse characteristics, the projected emittance and slice emittances goals remain well within the LCLS requirements for shot-to-shot pulses. In this paper, we present the PARMELA studies performed to design the LCLS photo-injector beamline and study its stability.

1 INTRODUCTION

Earlier optimizations of the LCLS photo-injector beamline had been done using a peak RF gun field of 140MV/m [3] [5], but operation at 120MV/m is less prone to RF breakdown at the cathode joint. A new optimization minimizing the emittance was desired.

Preliminarily, using Homdyn, the broad parameter space was explored to minimize the transverse emittance. Among the 19 free parameters, we only mention the laser spot size and time profile, solenoidal fields and position, injection phase, RF gun field and balance, accelerating structures ("linacs") position and gradient. For further optimization and more accurate space charge computation, systematic scans of those parameters were made using the LANL version of the PARMELA code interfaced to MATLAB around the operating point deduced from HOMDYN runs. A normalized projected emittance of 0.92 mm.mrad was obtained. For the new parameter list, a sensitivity study indicates very small deterioration of emittance with a variation of the solenoid current within power supply regulation tolerances and a relative stability with respect to the gun RF field.

Tolerances on emission pulse uniformities (transverse and longitudinal) are also discussed.

2 OPTIMIZATION

The beamline consists of an S-Band RF gun, with a copper photo-cathode, a first emittance compensation solenoid, two S-Band accelerating structures ("linac") and a second solenoid at the entrance of the first linac. The initial tuning with the gun operated at 140MV/m had been presented in the 1998 version of the LCLS CDR [5]. The optimal linac position had been found to be 1.4 m from the cathode [1] and the rms spot radius 1mm [3].

2.1 Nominal tuning

With a spot size radius of 1mm, and a linac gradient of 24MV/m in both sections, the linac section had to be moved from 1.4m to 2.2m from the cathode to reach a projected emittance smaller than 1 mm.mrad. This solution had 2 drawbacks:

- the beamline set-up was not flexible to accommodate operation at 140MV/m
- the longitudinal emittance was deteriorating along the drift space between gun and linac entrance

A better solution, keeping the linac at 1.4 m, was obtained but with a laser spot radius of 1.2 mm and a linac gradient slightly lower, namely 18.5 MV/m. The second linac section had to be tuned to 30.5 MV/m to have the electrons reach 150 MeV. The only disadvantage of this solution is that the thermal emittance which increases with radius will get slightly larger than in the previous tuning. The projected emittance for this new tuning is 0.92 / 1.03 mm.mrad for a pulse with 0.7 ps rise time and a thermal emittance of 0.3/ 0.6 mm.mrad. The main parameter values are summarized in the table below.

E_{gun} MV/m	$r_{spot\ size}$ mm	ϕ_{gun} /0-cros	B_{sol} kG	L0-2 MV/m	B_{sol} kG
120	1.2	27.8	2.71	18.5	0.8

Table 1: Parameters for new tuning

2.2 Slice emittance

In figure 1, the slice emittance values along the bunch are plotted for 100 slices for various thermal emittances. One hundredth of a bunch corresponds to slightly more than a cooperation length at the LCLS undulator location. For the 0.3 mm.mrad thermal emittance case, 97% of the particles are in slices with emittance smaller than 1 mm.mrad; 95 % of the particles are in slices with emittance smaller than 0.9 mm.mrad and 71% of the particles are in slices with emittance smaller than 0.8 mm.mrad. The matching parameter does not exceed 1.2 for 75 % of the beam. It was also checked using the 3D version of PARMELA-LANL that there is no emittance growth in the matching-diagnostics section where the beam aspect ratio becomes as large as 10:1.

2.2 Energy spread

According to PARMELA, the energy spread grows from 50 keV to 500 keV from the exit of the gun to the entrance of the linac. The uncorrelated energy spread is 7.10^{-4} for 80% (3.10^{-4} for 50%) of the slices at the core of the bunch. There are concerns that the correlated energy at the exit of the S-Band gun [7] would be larger than that computed by PARMELA. The source of this energy spread is still unknown. However, as an academic exercise, the beamline was optimized using an unbalanced gun. With a ratio of field amplitudes between the $\frac{1}{2}$ cell and the full cell of 0.8, the correlated energy spread at the exit of the gun is then of 125 keV but again 500 keV at the entrance of the linac. The minimum emittance was obtained when reducing the solenoid field by 3.5 % and the emittance increased only from 0.8 mm.mrad to 0.9 mm.mrad compared to the balanced gun case (with 0.35ps rise time and $\epsilon_{th} = 0.3$ mm.mrad thermal emittance).

3 SENSITIVITY

3.1 Individual parameters

The sensitivity of the projected emittance to errors in the tuning parameters was studied for the nominal case ($\epsilon_{th} = 0.3$ mm.mrad, 0.7ps rise time giving a projected emittance of 0.92 mm.mrad). First, the relative variation on a single parameter value necessary to increase the projected emittance from 0.92 mm.mrad to 1 mm.mrad was determined and is given in Table 2.

E_{c1}/E_{c2}	E_{gun}	ϕ_{gun}	B_{sol}	Q	r
3%	0.5%	$\pm 3^\circ$	$\pm 0.4\%$	+10%	8%

Table 2: Minimum variation of a single parameter value increasing ϵ_p from 0.92 to 1.0 mm.mrad. Parameters are: balance of gun (ratio field in the 2cells), amplitude field in

gun, injection phase, solenoid field, charge, spot size radius. The variation is given relative to the nominal value but for the injection phase given in degrees

3.2 Combination of errors

Second, the combination of those errors was studied. Sixty-four runs were generated combining the two extreme error values of the 6 parameters presented in Table 2. The degradation of projected emittance is presented in Table 3.

$\epsilon < 1$	$1 < \epsilon < 1.2$	$1.2 < \epsilon < 1.5$	$1.5 < \epsilon < 2$	$\epsilon > 2$
13	26	12	10	3

Table 3: Combination of errors; number of runs (out of 64) with projected emittance ϵ (mm.mrad) fulfilling inequality in row 1

Those sixty-four cases correspond to extreme cases. A real statistical study could be performed if enough CPU time was used. Very few of these cases give emittances below one however, the worst case which corresponds to a projected emittance of 2.5 mm.mrad has a rather good slice emittance. For 80% of the slices, the slice emittance is below 1.2 mm.mrad.

3.3 Jitter errors

Stability on parameters to be obtained from shot-to-shot is much smaller than what was used in 3.2. To perform a jitter study we used offset values which are only very slightly larger than design tolerances (Table 4).

E_{c1}/E_{c2}	E_{gun}	ϕ_{gun}	B_{sol}	Q	r
$\pm 3\%$	$\pm 0.3\%$	$\pm 0.5^\circ$	$\pm 0.01\%$	2%	8%

Table 4: Values used for jitter error study (slightly larger than specified tolerances)

The variation is now dominated by the field balance and field amplitude values. The distribution of projected emittance values is given in Table 5. The worst case gives a projected emittance of 1.25 mm.mrad. However, 90% of the slices have emittance values still below 0.9 mm.mrad.

$\epsilon < 0.95$	$0.95 < \epsilon < 1$	$1 < \epsilon < 1.1$	$1.1 < \epsilon < 1.2$	$\epsilon > 1.2$
17	23	11	11	2

Table 5: Combination of errors; number of runs (out of 64) with projected emittance ϵ (mm.mrad) fulfilling inequality in row 1

4 TOLERANCES

All the previous PARMELA runs discussed here above have been done using a 10ps pulse with 0.7 ps rise time a thermal emittance of 0.3 mm.mrad and a flat uniform transverse profile. The operation of test facilities using S-Band photo-cathode guns [7] has demonstrated the importance of using realistic emission distribution to simulate the beam. Tighter tolerances than those achieved until now, but realistic, have been defined for the LCLS photo-injector and are justified in this chapter.

4.1 Thermal emittance

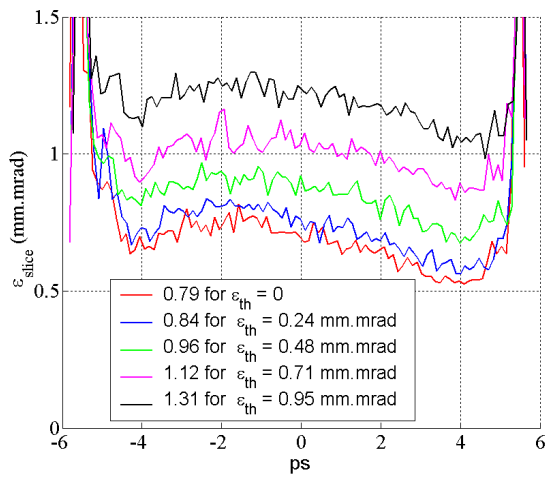


Figure 1. Slice emittance along bunch at the end of beamline for various thermal emittances.

The thermal emittance varies linearly with radius. Measurements indicate that for a copper cathode the thermal emittance is of 0.3 to 0.6 mm.mrad per mm radius [7]. Using the worst case, the thermal emittance for a 1.2 mm radius spot size would be 0.72 mm.mrad. The projected emittance is then 1.12 mm.mrad. In figure 1, the slice emittance along the bunch has been plotted for different thermal emittances. The projected emittance for those cases is indicated in the legend. It follows a quadratic law of the thermal emittance. The thermal emittance model used here is a Gaussian distribution of angular velocities.

4.2 Longitudinal profile

a- Rise time

The longitudinal emission profiles used in the PARMELA simulations to provide flat tops are built by stacking Gaussians. The rise time of the flat top distribution is given by the rms value of the unit Gaussian, The slice emittance is obviously not affected by the change in rise time, but the projected emittance deteriorates rapidly as

presented in Figure 2. A 0.7 ps rise time can easily be achieved with the Ti-Sapphire laser presently designed for the LCLS. The system is capable of achieving rise times of 0.3 ps.

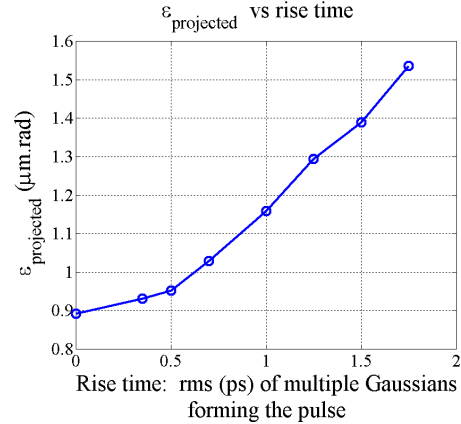


Figure 2- Projected emittance vs rise time (computed for thermal emittance of 0.6mm.mrad)

b- Modulation of density

A modulation on top of a square longitudinal profile does not produce any emittance increase. The amplitude of modulation needs to be as large as 65 % to notice a small difference in slice emittance. The modulation is already partly washed out at the exit of the gun. The correct computation of high charge densities would require including Shottky effect and tests on space charge limit.

4.3 Transverse emission spot

The uniformity of the transverse emission spot results from the uniformity of the laser and that from the cathode emission surface. We studied the case of an emission spot modeled with a rectangular density grid of the checker board type. This case requires the use of the 3D algorithm from PARMELA-LANL. It is highly CPU time consuming and requires running at least 100 000 macro-particles. Results are given in Figure3. An experimental study of such a distribution has been initiated [8].

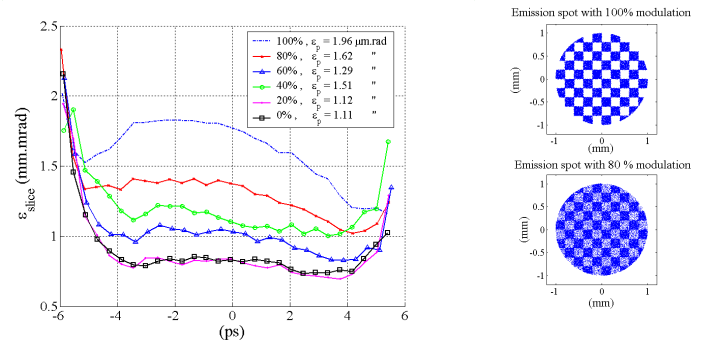


Figure 3- Slice emittance for different modulation of the densities on emission spot; $r = 1\text{mm}$; $\epsilon_{th} = 0.3\text{ mm.mrad}$.

5 CONCLUSION

PARMELA-LANL simulations used to design the LCLS photo-injector beamline has been presented. Computations show that this beamline will produce a 150MeV, 1nC, 10 ps pulse with a 1.2 mm.mrad projected emittance and slice emittances below 1.0 mm.mrad in the presence of errors and with a thermal emittance of 0.7 mm.mrad. Tolerances for pulse rise time and transverse emission spot uniformity have been defined. This beamline also has a great flexibility. It can accommodate the operation of the gun with field amplitude ranging from 120MV/m to 140MV/m. A tuning for a gun unbalanced by 20% was also demonstrated. The computations rely on LANL-PARMELA. Efforts have been made to benchmark the code with respect to experiment [7] and with respect to PIC codes [4].

Acknowledgements

The authors are very grateful to L.Young for his very valuable support on PARMELA. They would like to thank E.Colby and P.Emma for their many advice and exciting discussions on the physics. They also thank M.Ferrario and J.Lewellen for their help respectively on Homdyn and PARMELA. They are grateful to M.Cornacchia and J.Galayda for their support. This work was supported by the Department of Energy under contract DE-AC03-76SF00515.

6 REFERENCES

- [1] M.Ferrario, "Homdyn Study for the LCLS RF Photo-Injector", SLAC PUB 8400, March 2000
- [2] W.Graves et al. "Measurement of Thermal Emittance for a Copper Photocathode ", Proceedings PAC 2001
- [3] D.Palmer "The next generation PhotoInjector", PhD Manuscript , June 1998
- [4] E.Colby, Private Communication, "Task Force on comparison between PIC code and PARMELA "
- [5] LCLS CDR December 1998 Revision, <http://www-ssrl.slac.stanford.edu/lcls/>
- [6] LCLS CDR April08-2002, <http://www-ssrl.slac.stanford.edu/lcls/CDR/>
- [7] C.Limborg et al. "PARMELA Simulations against experiments at the GTF and SDL Facilities", these proceedings
- [8] I.B.Zvi et al. "Experimental Studies of Emittance Growth Due to Laser Non-uniformity", these proceedings